T cell receptor specificity drives accumulation of a reparative population of regulatory T cells within acutely injured skeletal muscle

Jun Cho[a,b,c], Wilson Kuswanto[a,b,1], Christophe Benoist[a,b], and Diane Mathis[a,b,2]

[a]Department of Immunology, Harvard Medical School, Boston, MA 02115; [b]Evergrande Center for Immunologic Diseases, Harvard Medical School and Brigham and Women's Hospital, Boston, MA 02115; and [c]Department of Biomedical Science and Engineering, Gwangju Institute of Science and Technology, 61005 Gwangju, South Korea

Contributed by Diane Mathis, October 29, 2019 (sent for review August 27, 2019; reviewed by Marco Colonna and Jeffrey V. Ravetch)

Foxp3$^+$CD4$^+$ regulatory T cells (Tregs) play important roles in controlling both homeostatic processes and immune responses at the tissue and organismal levels. For example, Tregs promote muscle regeneration in acute or chronic injury models by direct effects on local muscle progenitor cells, as well as on infiltrating inflammatory cells. Muscle Tregs have a transcriptome, a T cell receptor (TCR) repertoire, and effector capabilities distinct from those of classical, lymphoid-organ Tregs, but it has proven difficult to study the provenance and functions of these unique features due to the rarity of muscle Tregs and their fragility on isolation. Here, we attempted to sidestep these hindrances by generating, characterizing, and employing a line of mice carrying rearranged transgenes encoding the TCRα and TCRβ chains from a Treg clone rapidly and specifically expanded within acutely injured hindlimb muscle of young mice. Tregs displaying the transgene-encoded TCR preferentially accumulated in injured hindlimb muscle in a TCR-dependent manner both in the straight transgenic model and in adoptive-transfer systems; non-Treg CD4$^+$ T cells expressing the same TCR did not specifically localize in injured muscle. The definitive muscle-Treg transcriptome was not established until the transgenic Tregs inhabited muscle. When crossed onto the *mdx* model of Duchenne muscular dystrophy, the muscle-Treg TCR transgenes drove enhanced accumulation of Tregs in hindlimb muscles and improved muscle regeneration. These findings invoke the possibility of harnessing muscle Tregs or their TCRs for treatment of skeletal muscle pathologies.

regulatory T cell | T cell receptor | transgenic mice | skeletal muscle | tissue repair

Foxp3$^+$CD4$^+$ regulatory T cells (Tregs) are pivotal regulators of diverse types of immune responses (e.g., autoimmunity, allergy, reactions to infection, and antitumor immunity) (1). Tregs can suppress abnormal immune responses by downregulating the activities of T cells, B cells, or several elements of the innate immune system. More recently, a second role for Tregs has been uncovered: control of organismal homeostasis (2). Analogous to previous findings on macrophages (3, 4), Tregs localized in a variety of tissues have been found to influence the activities of neighboring parenchymal cells to maintain optimum tissue function. For example, a unique population of Tregs residing in visceral adipose tissue (VAT) regulates metabolic indices as well as the local and systemic inflammatory state (5), and a different population of Tregs in skeletal muscle promotes tissue regeneration on acute or chronic injury (6).

Two features subtend the unique phenotypes and functions of tissue-Tregs: distinct transcriptomes and clonally expanded T cell receptor (TCR) repertoires (5–7). Their transcriptomes differ by hundreds to thousands of transcripts from those of both lymphoid-organ Tregs and Tregs localized within other nonlymphoid tissues. Certain of the differentially expressed transcripts, such as those encoding PPARγ in VAT Tregs (8) or Areg in muscle Tregs (6), play an important role in driving the accumulation or functional activities of tissue-Tregs. T cell repertoire analyses revealed clonal expansions of Tregs expressing specific TCRs in nonlymphoid tissues. This finding suggested that local interactions between TCRs and particular tissue antigens might be responsible for the accumulation, and eventually the phenotype, of tissue-Tregs, a notion that was recently confirmed for VAT (9).

Skeletal muscle, the largest vertebrate organ, has a highly specialized structure composed primarily of postmitotic, multinucleate cells (myofibers). On injury, muscle follows a robust regeneration program to reconstitute damaged myofibers (10). This process is accompanied by accumulation of various types of immune system cells through both proliferation and recruitment (11). For example, Tregs are substantially enriched in both acutely and chronically injured muscle, constituting 40 to 60% of the CD4$^+$ T cell compartment, a much higher frequency than the typical circulating Treg frequency of 10 to 15% (6). Ablation or augmentation of Tregs in mice results in a compromised or enhanced muscle regeneration response, respectively (6, 12, 13). In aged mice, the accumulation of muscle Tregs on acute injury is subpar, resulting in a dampening of reparative capacity (12). Expansion of muscle Tregs by administration

Significance

Regulatory T cells (Tregs) with a distinctive transcriptome and T cell receptor (TCR) repertoire regulate muscle repair in injury models. Important issues concerning muscle-Treg biology remain unresolved because of their rarity and fragility on isolation. To circumvent these problems, we generated transgenic mice carrying rearranged *Tcra* and *Tcrb* genes from a Treg clone expanded within muscle after injury. The TCR transgenic mice had a TCR repertoire skewed for the transgene-encoded specificity and an amplified population of muscle Tregs. The tissue accumulation, phenotype acquisition, and functional activities of muscle Tregs were critically dependent on TCR specificity. Introduction of the TCR transgenes into a model improved muscle regeneration, suggesting a therapeutic potential for muscle Tregs or their TCRs.

Author contributions: J.C. and D.M. designed research; J.C. and W.K. performed research; J.C., C.B., and D.M. analyzed data; J.C. and D.M. wrote the paper; and C.B. and D.M. supervised research.

Reviewers: M.C., Washington University School of Medicine in St. Louis; and J.V.R., Rockefeller University.

The authors declare no competing interest.

Data deposition: The data reported in this paper have been deposited in the Gene Expression Omnibus (GEO) database, https://www.ncbi.nlm.nih.gov/geo (accession no. GSE140419).

[1]Present address: Department of Medicine, Stanford University Medical Center, Stanford, CA 94305.

[2]To whom correspondence may be addressed. Email: cbdm@hms.harvard.edu.

This article contains supporting information online at https://www.pnas.org/lookup/suppl/doi:10.1073/pnas.1914848116/-/DCSupplemental.

First published December 10, 2019.

of interleukin 33, a tissue-Treg growth and maintenance factor, enhances tissue repair in aged mice.

Several important issues concerning muscle-Treg biology remain unresolved. Notably, when and where do muscle Tregs acquire their unique features? Furthermore, can they be harnessed therapeutically to ameliorate muscle diseases? Major hurdles to addressing these questions have been the scarcity and fragility of muscle Tregs, problems exacerbated by the isolation procedures required to release them. To circumvent these hindrances, we constructed a transgenic (tg) mouse line carrying the rearranged *Tcra* and *Tcrb* genes encoding the TCR displayed by a muscle-Treg clone expanded in multiple mice shortly after injury. The TCR-tg mice had a T cell repertoire highly skewed for the transgene-encoded specificity, and consequently, an amplified population of muscle Tregs. Exploiting this model, we demonstrated that the tissue accumulation, phenotype acquisition, and functional activities of muscle Tregs were dependent on TCR specificity. We also showed that introduction of the TCR transgenes into a mouse model of Duchene muscular dystrophy improved muscle regeneration, thereby supporting the therapeutic potential of muscle Tregs for degenerative muscle diseases.

Results

Construction and Characterization of mTreg24, a Muscle-Treg TCR-tg Mouse Line. In a previous study (6), we identified multiple Treg clones that accumulated in the hindlimb muscles of C57BL/6J (B6) mice soon after cardiotoxin (Ctx)-induced injury. Among these, we chose mTreg24 for the construction of a TCR-tg mouse line for several reasons. First, although expanded tissue-Treg clones are usually private [i.e., almost never detected in more than 1 mouse (6, 7)] mTreg24 (or a clone displaying a TCR with a single conservative amino acid substitution) was found in 11 individual mice 2 or 4 d, but not 8 day, after Ctx-induced injury. Second, mTreg24 expressed Vα3.2 and Vβ8.2 variable regions, and monoclonal antibodies capable of recognizing $V\alpha3^+$ and $V\beta8^+$ TCR chains were commercially available. Genomic DNA constructs encompassing the rearranged *Tcra* and *Tcrb* genes from this clone were generated, cloned, and injected into B6 mouse embryos. A muscle Treg TCR-tg mouse, mTreg24, was identified among the offspring and was bred to establish a line.

Initially, we examined Treg populations in mTreg24 tg mice on the standard B6 genetic background. Tg^+ mice had a significantly greater number of muscle Tregs 3 d after Ctx injury than their Tg^- littermates had (Fig. 1*A*). Treg frequencies (as a percentage of $CD4^+$ T cells) in the muscles of Tg^+ and Tg^- mice were quite similar likely because the number of conventional T cells (Tconvs) in the tg line was also elevated, reflecting the typical muscle-induced inflammatory response in the context of incomplete allelic exclusion of the transgene-encoded TCR, especially in Tconvs (*SI Appendix*, Fig. S1). In contrast, Tg^+ and Tg^- littermates had similar numbers and frequencies of Tregs in the spleen.

Because we found that the commercially available anti-Vα3 monoclonal antibody (mAb) did not in fact detect the mTreg24 TCRα chain, our quantification of Tregs expressing the transgene-encoded TCR was limited to detection of $V\beta8^+$ TCRs. Both the frequency and number of $V\beta8^+$ Tregs were highly elevated in the 3-d Ctx-injured muscle of Tg^+ compared with Tg^- littermates; a less striking increase was found in the corresponding spleens (Fig. 1*B*). A useful measure of relative enrichment is the ratio of $V\beta8^+$ Treg numbers in the muscle and spleen of Tg^+ vs. Tg^- littermates: 5- to 10-fold higher in muscle (Fig. 1*C*). Preferential accumulation of $V\beta8^+$ Tregs was found throughout the time-course of Ctx-induced injury in the TCR-tg mice (Fig. 1 *D*, *Upper*). Notably, the fractions of $V\beta8^+$ Tregs in uninjured muscle and spleen of mTreg24 mice were both about 8%, arguing that the build-up of Tregs within muscle was injury-induced. $V\beta8^+$ Tconv cells favored the spleen rather than injured muscle of TCR-tg mice (Fig. 1 *D*, *Lower*), emphasizing the specificity of $V\beta8^+$ Treg accumulation in muscle.

To specifically track Tregs expressing the transgene-encoded TCR (in the absence of an appropriate anti-Vα3 mAb), we crossed the mTreg24 transgenes onto a B6.$Rag^{-/-}$ genetic background. The frequency of Tregs in hindlimb muscles of these mice rose to 70 to 80% on injury, which was substantially higher than that of control littermates (Fig. 1*E*). Spleens showed the opposite result: lower Treg frequencies in Tg^+ than Tg^- mice. Tconvs did not preferentially accumulate in injured muscle of mTreg24 tg mice on the B6.$Rag^{-/-}$ background (Fig. 1*E*).

In brief, we successfully generated a muscle Treg TCR-tg mouse line with enhanced Treg accumulation in skeletal muscle on acute injury. This behavior was particularly true of Tregs displaying the transgene-encoded TCR.

Accumulation of Muscle Tregs Was Dependent on the TCR Specificity. The preferential accumulation of $V\beta8^+$ Tregs in injured hindlimb muscles of mTreg24 tg mice suggested that the TCR specificity is a critical driver of muscle Treg enrichment on injury. However, this conclusion might be questioned because of the inability to identify Tregs expressing only the transgene-encoded TCR in TCR-tg mice on the standard B6 background and because of the lymphopenic status of TCR-tg mice on the B6.$Rag^{-/-}$ background. Therefore, we turned to an adoptive-transfer approach (Fig. 2*A*).

In a first set of experiments, total $CD4^+$ T cells were isolated from pooled spleen and lymph nodes of Tg^- B6.CD45.2.$Rag^{+/+}$ or Tg^+ B6.CD45.2.$Rag^{-/-}$ donors, and were transferred into Tg^- B6.CD45.1/2.$Rag^{+/+}$ recipients. Hindlimb muscles of recipient mice were Ctx-injured 7 d after adoptive transfer, and were analyzed 3 d later. The frequencies of polyclonal Tg^- donor cells within the muscle and spleen $CD4^+$ T cell compartments of recipient mice were not statistically different, whereas the frequency of contemporaneously transferred monoclonal Tg^+ donor cells was 5 to 10 times higher in muscle than in spleen (Fig. 2*B*). Thus, there was a strong relative enrichment of $CD4^+$ T cells expressing the transgene-encoded TCR within injured muscle (vis-à-vis spleen; Fig. 2*C*). Moreover, there was an overabundance of Tg^+, but not Tg^-, donor Tregs within the $CD4^+$ T cell compartment of injured muscle from recipient mice, an enrichment that was much less evident in the spleen (Fig. 2 *D* and *E*). The minimal enrichment of Tg^+ donor cells in other nonlymphoid organisms, such as the lung, liver, or kidney, was similar to that in the spleen (*SI Appendix*, Fig. S2). Similar results were obtained when Ctx was administered 2 d before the adoptive transfer of $CD4^+$ T cells (*SI Appendix*, Fig. S3).

These findings establish that the TCR specificity critically influenced Treg accumulation in injured muscles. Tregs displaying the mTreg24 TCR were much more prone to populate damaged muscles than were polyclonal Tregs.

The Definitive Muscle-Treg Transcriptome Is Set in the Muscle. Muscle Tregs have a transcriptome distinct from those of lymphoid-tissue Tregs and of Tregs within other nonlymphoid tissues (6, 14). Given their rarity and fragility on isolation, it has not been possible to ascertain where muscle Tregs acquire their distinct nature. Transcriptomic analysis of Treg populations in mTreg24 tg mice should shed light on this issue, as the myophilic Treg clone can be captured in both muscle and lymphoid tissue of the same mouse. Thus, we performed ultralow-input RNA-seq analysis on double-sorted $V\beta8^+$ or total Tregs from the hindlimb muscle and spleen 3 d after Ctx-induced injury of Tg^+ or Tg^- mice, respectively.

Overlaying our previously reported muscle Treg signature (6) onto a volcano-plot (*P* value vs. fold-change) comparison of muscle and spleen Tregs from injured TCR-tg mice revealed heavy skewing of both the "up" and "down" components in muscle Tregs, including diagnostic transcripts such as *Areg*, *Il1rl1*, *Il10*, *Cxcr5*, and *Tcf7* (Fig. 3*A*). The muscle:spleen differential transcripts have been detailed previously (6, 12); as expected, pathway analysis showed an enrichment for inflammation-related topics (*SI Appendix*, Fig.

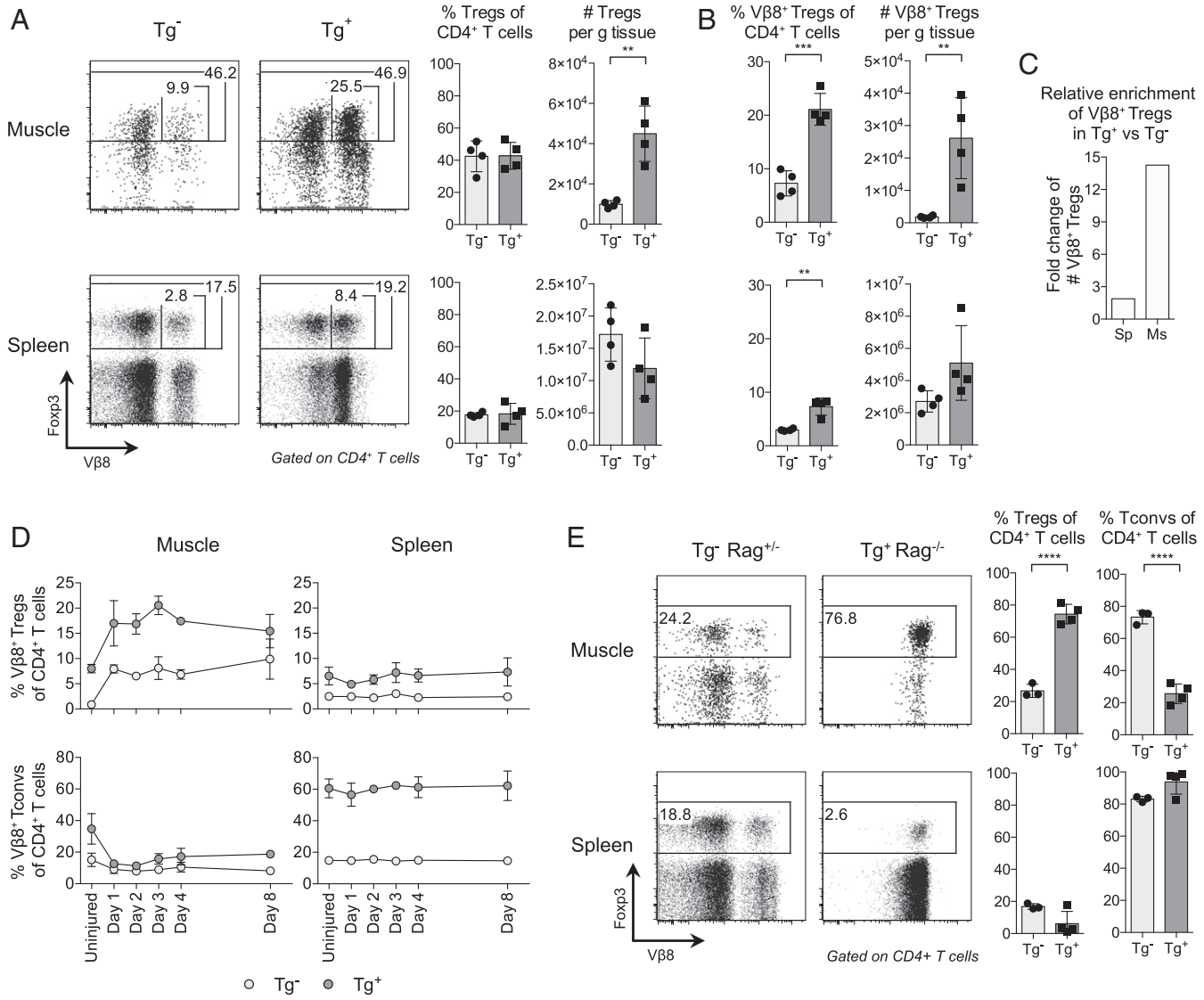

Fig. 1. Characterization of Tregs in mTreg24 tg mice. Flow cytometric analyses of CD4$^+$ T cell compartments from hindlimb muscles and spleens of 3-d Ctx-injured TCR-tg and non-Tg littermates. (*A*) Representative dot-plots, Treg frequencies, and Treg numbers for 8-wk-old mice, $n = 4$. (*B*) Vβ8$^+$ Treg frequencies and numbers for the same mice. (*C*) Relative enrichment of Vβ8$^+$ Tregs in Tg$^+$ vs. Tg$^-$ mice. $n = 4$. (*D*) Frequencies of Vβ8$^+$ Tregs and Tconv cells at various points after injury. $n = 2$ to 6. (*E*) Representative dot-plots and frequencies for Tregs and Tconvs from 10-wk-old Tg$^-$ B6.*Rag*$^{+/-}$ mice and Tg$^+$ B6.*Rag*$^{-/-}$ littermates, day 3 after Ctx injury. For all panels: mean ± SD $^*P < 0.05$; $^{**}P < 0.01$; $^{***}P < 0.001$; $^{****}P < 0.0001$ by the unpaired, 2-tailed Student's *t* test.

S4*A*). Flow cytometric analysis (*SI Appendix*, Fig. S4 *B* and *C*) confirmed higher protein expression in the cases of ST2 (encoded by *Il1rl1*) and CD103 (*Itgae*). Two previously reported T cell activation signatures (15, 16) were highly overrepresented in the muscle, compared with spleen, transcriptome (Fig. 3*B*), suggesting that these cells did not undergo final antigenic activation until localized within muscle. Notably, the muscle Treg "up" and "down" components were more strongly represented in muscle Tregs from Tg$^+$ than Tg$^-$ mice (Fig. 4*D*), likely due to the latter's polyclonal nature, including tourist TCR specificities just passing through.

mTreg24 tg Tregs Enhanced Muscle Regeneration in a Muscular Dystrophy Model. On the basis of previous reports (6, 12, 13), we anticipated that the elevated number of muscle Tregs in Ctx-injured TCR-tg mice, with their augmented expression of transcripts encoding reparative factors such as interleukin 10 and Areg, would enhance muscle repair. Indeed, a previously established Areg-induced signature (6) was significantly skewed in the whole-muscle transcriptome of Tg$^+$ vs. Tg$^-$ littermates 8 d after Ctx injection (*SI Appendix*, Fig. S5*A*). However, we did not detect any significant changes in the inflammatory infiltrate or in myofiber regeneration in analogous comparisons.

Reasoning that the benefits of transgene expression under this relatively short-term protocol might be limited, we turned to a longer-term, pathological model of muscle injury, crossing the mTreg24 *Tcr* transgenes onto the *mdx* genetic background, a dystophin-deficient mouse line that models Duchenne muscular dystrophy. We had previously demonstrated a mitigating role for muscle Tregs in this model (6). Both at 4 and 12 wk of age (the acute and chronic stage, respectively), there was a preferential accumulation of Vβ8$^+$ TCR-tg Tregs in skeletal muscle (Fig. 4 *A* and *B*). Leukocyte infiltration was not significantly different in Tg$^+$ and Tg$^-$ *mdx* littermates (*SI Appendix*, Fig. S5*B*), nor was accumulation of macrophages or their pro- to antiinflammatory transition (*SI Appendix*, Fig. S5 *C* and *D*). However, in 12-wk-old

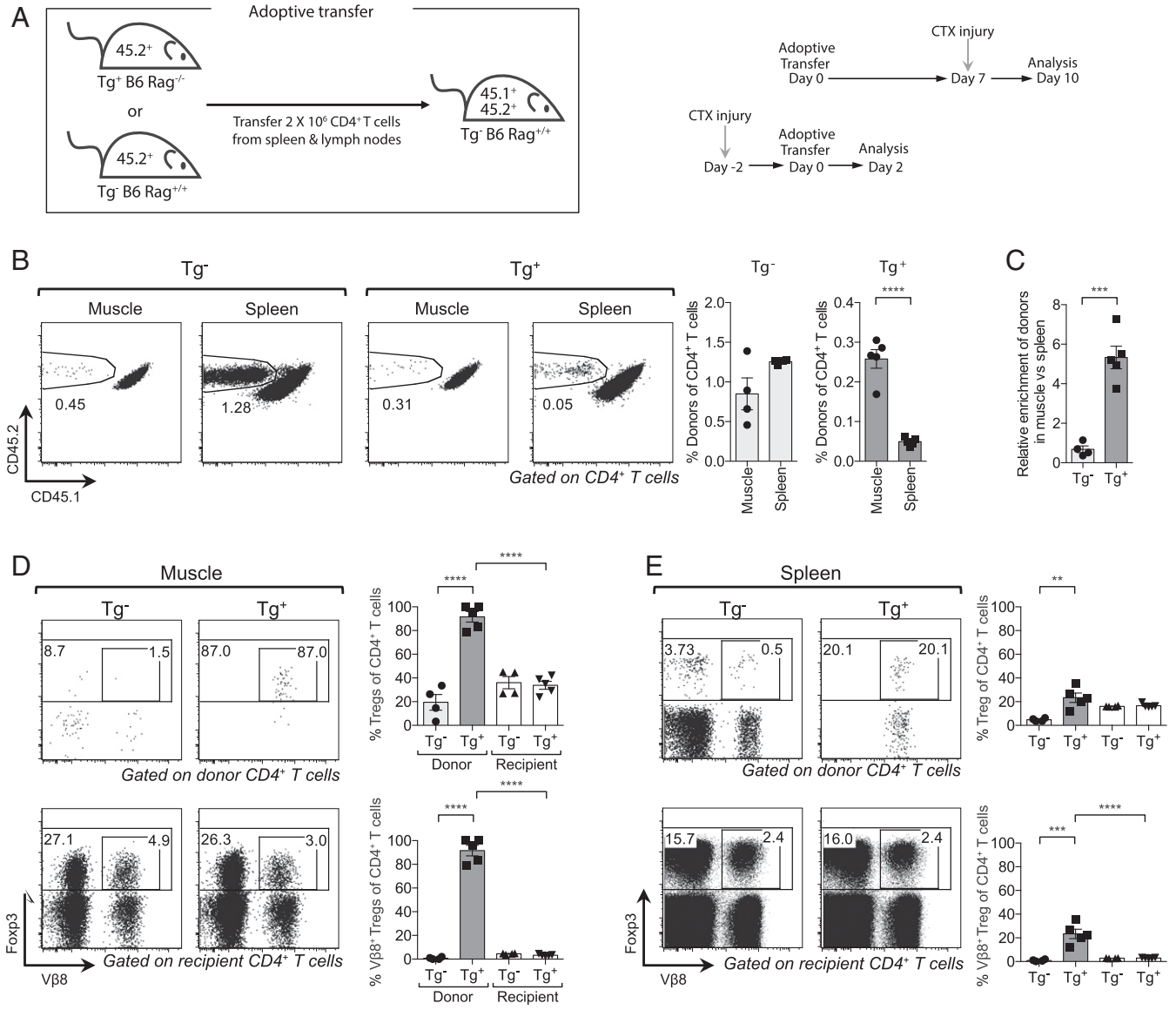

Fig. 2. Muscle Treg accumulation depended on their TCR specificity. (*A*) Adoptive transfer protocols. Donor CD4$^+$T cells were isolated from pooled spleen and lymph nodes of TCR-tg B6.CD45.2$^+$.*Rag*$^{-/-}$ mice or nontg B6.CD45.2$^+$.*Rag*$^{+/+}$ mice and transferred into Tg$^-$ B6.CD45.1/2*Rag*$^{+/+}$ recipients. (*B*) Representative dot-plots and frequencies for Tg$^+$ or Tg$^-$ CD45.2$^+$ donor cells among total CD4$^+$ T cells of recipient mice muscles and spleens, 10 d after the adoptive transfer, 3 d after Ctx injury. (*C*) Relative enrichment of donor cells in muscle vs. spleen. (*D*) Representative dot-plots, fractions of donor Tregs among donor and recipient CD4$^+$ T cells, and fractions of Vβ8$^+$ donor Tregs within their compartments for muscle 10 d after adoptive transfer. (*E*) Same as in *D* except spleen. Statistics as per Fig. 1. $^{**}P < 0.01$, $^{***}P < 0.001$, $^{****}P < 0.0001$; $n = 5$.

mice, the distribution and mean cross-sectional area of regenerating myofibers with centralized nuclei were clearly increased in muscle of Tg$^+$ mice (Fig. 4 *D* and *E* and *SI Appendix*, Fig. S5*E*), indicating that they were at a more advanced stage of regeneration.

Discussion

Our previous observation that certain muscle Treg clones expand on Ctx-induced injury (6) suggested that TCR recognition of a local antigen might be the driver of their accumulation. Since other explanations are also possible, we generated and employed a line of muscle-Treg TCR-tg mice (mTreg24) to directly address this issue. Indeed, enhanced accumulation of muscle Tregs in both the straight TCR-tg and adoptive transfer systems, in particular in the *Rag*$^{-/-}$ context, argued for a critical role for TCR specificity in driving muscle-Treg localization. An analogous conclusion came from a recent study employing VAT-Treg TCR-tg mice, in which an expanded VAT Treg population dominated by cells expressing the transgene-encoded TCR was observed (9). In both tissue contexts, it seems that the role of the TCR, through its engagement of MHC:peptide complexes, is to promote proliferation of tissue-localized Tregs, and above all, their retention within the appropriate tissue. Other factors (e.g., cytokines) also play a role in tissue-Treg proliferation, as has been demonstrated for interleukin 33 in both VAT and muscle (7, 12).

Also analogous to the VAT-Treg TCR-tg mice, Foxp3$^-$CD4$^+$ Tconv cells displaying the transgene-encoded TCR on a *Rag*$^{-/-}$ background failed to accumulate in the target tissue even though they expressed exactly the same TCR as the Tregs that did accumulate. The missing factor is likely Foxp3, itself, as previously established for VAT Tconv cells, where it was found to induce expression of several homing receptors and survival factors (9).

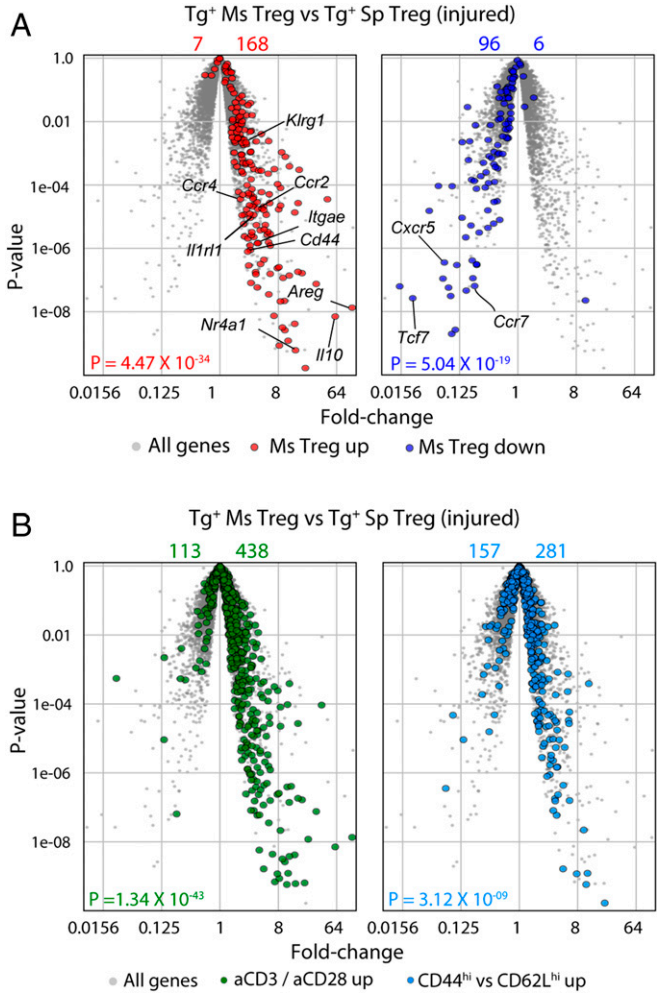

Fig. 3. TCR specificity drove acquisition of the muscle-Treg transcriptome. Transcriptomic analyses of Tregs from hindlimb muscles and spleens of 8-wk-old TCR-tg mice and nontg controls. Vβ8$^+$ Tregs (for Tg$^+$ mice) or total Tregs (for Tg$^-$ mice) were isolated from muscle (Ms) or spleen (Sp) of mTreg24/Foxp3-GFP mice and nontg littermates 3 d after Ctx-induced hindlimb injury. (*A*) Volcano plots comparing the transcriptomes of injured Ms and Sp Tregs from Tg$^+$ mice. An established muscle-Treg signature (6) is overlain in red (up-component, *Right*) or blue (down-component, *Left*). (*B*) Two previously reported T cell activation signatures (15, 16) overlain on the same datasets, depicted as green or light-blue dots. For all plots: duplicates per condition. *P* values according to the χ^2 test.

Although, as tissue-Tregs, muscle- and VAT-Tregs share many features, several observations indicate that they also have distinct aspects. For example, in the adoptive transfer experiments, donor mTreg24 Tregs expanded in injured muscles much more rapidly than donor vTreg53 Tregs did in VAT, and the expansion seemed less durable in the former case. It is possible that muscle Tregs have a limitation on their establishment in undamaged muscle. Given that they rapidly proliferate in response to injury, tissue damage may permit them to overcome this restriction and accumulate in the vicinity of the damaged site. This speculation raises the question of what kind of antigen or antigens muscle Tregs recognize: are they muscle-specific, injured-muscle-specific, or just injury-specific?

Transcriptomic comparison of muscle Tregs from Tg$^+$ and Tg$^-$ littermates revealed the former to have the stronger muscle-Treg phenotype, as represented by our previously reported muscle-Treg signature (6). Given that these observations emanated from population-level RNA-seq analysis, they could indicate that individual cells within the population had a more robust muscle-Treg phenotype or, alternatively, that a higher fraction of cells within the population had the typical muscle-Treg phenotype. Notably, despite the overall over- and underrepresentation of the muscle Treg up- and down-signatures, respectively, in Tg$^+$ vs. Tg$^-$ littermates, certain genes appeared to be discordantly down- or up-regulated in Tg$^+$ muscle Tregs (e.g., *Il10*). This outcome might be attributable to selective expansion of a particular subpopulation of muscle Tregs in the TCR-tg mice.

Last, the improvement in muscle regeneration in *mdx* mice carrying the mTreg24 transgenes highlights the potential of harnessing muscle Tregs or their products for therapeutic ends. The important role of a muscle-Treg TCR in driving the accumulation and phenotypic specialization of this unique population evokes the potential of TCR grafting approaches, which are increasingly pursued in contexts of tumorigenesis and infection (17).

Materials and Methods

Mice. C57BL/6 (B6), B6.SJL-*Ptprc^{a}Pepc^b*/BoyJ (B6.45CD45/1$^+$, #002014), and C57BL/10ScSN-*Dmd^{mdx}*/J (mdx, #001801; *mdx*) mice were purchased from Jackson Laboratory. B6.*Foxp3-GFP* (Foxp3-GFP) mice were obtained from V. Kuchroo, Brigham and Women's Hospital, Boston, MA.

For generation of the mTreg24 TCR-tg line, DNA fragments encoding the rearranged TCRα (TRAVD-4*04F/TRAJ30*01F, CDR3 sequence CAVSNNAGAKLTF), and TCRβ *TRBV13-2*05F/TRBJ2-7*01F, CDR3 sequence: CASGDEQYF) chains were synthesized by Integrated DNA Technologies and cloned into the pTacass and pTbcass, respectively, TCR-transgene vectors (18). The resulting constructs were amplified in *Escherichia coli* and excised to remove prokaryotic expression modules and to linearize. DNA fragments were purified and coinjected into fertilized B6 eggs to obtain founders expressing the transgene-encoded TCR. Validation of the genotype was via polymerase chain reactions amplifying the rearranged DNA sequences. TCR-tg mice were further crossed with Foxp3-GFP, *Rag*$^-$, or *mdx* mice. All experiments were conducted under protocols approved by Harvard Medical School's Institutional Animal Care and Use Committee.

Acute Muscle Injury. Mice were anesthetized with Avertin (0.4 mg/g body weight) and injected with *Naja mossambica* Ctx (300 ng per muscle) into 1 or more hindlimb muscles (TA, gastrocnemius, and quadriceps).

Isolation of Leukocytes from Nonlymphoid Tissues. Hindlimb muscles were minced and digested at 37 °C for 30 min in Dublecco's modified Eagle medium (DMEM) without phenol red, containing collagenase II (2 mg/mL; Thermo Fisher Scientific) and DNase I (150 μg/mL; Sigma-Aldrich) underlain with 80% Percoll, and spun for 25 min at 1,126 × *g*. The interphase containing leukocytes was carefully isolated and washed with DMEM containing 2% FBS and stained for flow cytometric analysis or sorting. Leukocytes from lung, liver, and kidney were isolated according to protocols described previously (19).

Adoptive Transfer of CD4$^+$ T Cells. Donor CD4$^+$ T cells were isolated from pooled spleens and lymph nodes of 8-wk-old male Tg$^+$ CD45.2$^+$ Rag$^{-/-}$ mice or wild-type B6 mice, using Dynabeads Untouched Mouse CD4 Cells Kit (Thermo Fisher Scientific). 2 × 10^6 cells were retro-orbitally administered to each 6- to 8-wk-old CD45.1/2$^+$ B6 male recipient. The hindlimb muscles of recipients were injured with Ctx at the aforementioned times. Two or 3 d after Ctx injury, leukocytes were purified from muscle and spleens of the recipients and stained for flow-cytometric analyses.

RNA-Seq Library Preparation and Sequencing. For RNA-seq library construction, Vβ8$^+$ Tregs or total Tregs were double-sorted by Moflo from muscle and spleen of Tg$^+$ or Tg$^-$, respectively, Foxp3-GFP mice 3 d after Ctx-injury. 2 × 10^3 cells were lysed with TCL buffer (Qiagen) containing 1% 2-mercaptoethanol (Sigma) and used for generating libraries as previously described (20). For whole-muscle RNA-seq library construction, muscles of Tg$^+$ or Tg$^-$ mice were collected 8 d after Ctx injury. Total RNAs were isolated using TRIzol (Invitrogen) according to the manufacturer's instructions. Five nanograms RNA was used for generating each library, as above. Sequencing was performed on an Illumina NextSeq500, using the 2 × 25 base pair read option. Transcripts were quantified via the Broad Technology Labs computational pipeline (21). Subsequent analyses were carried out using in-house software.

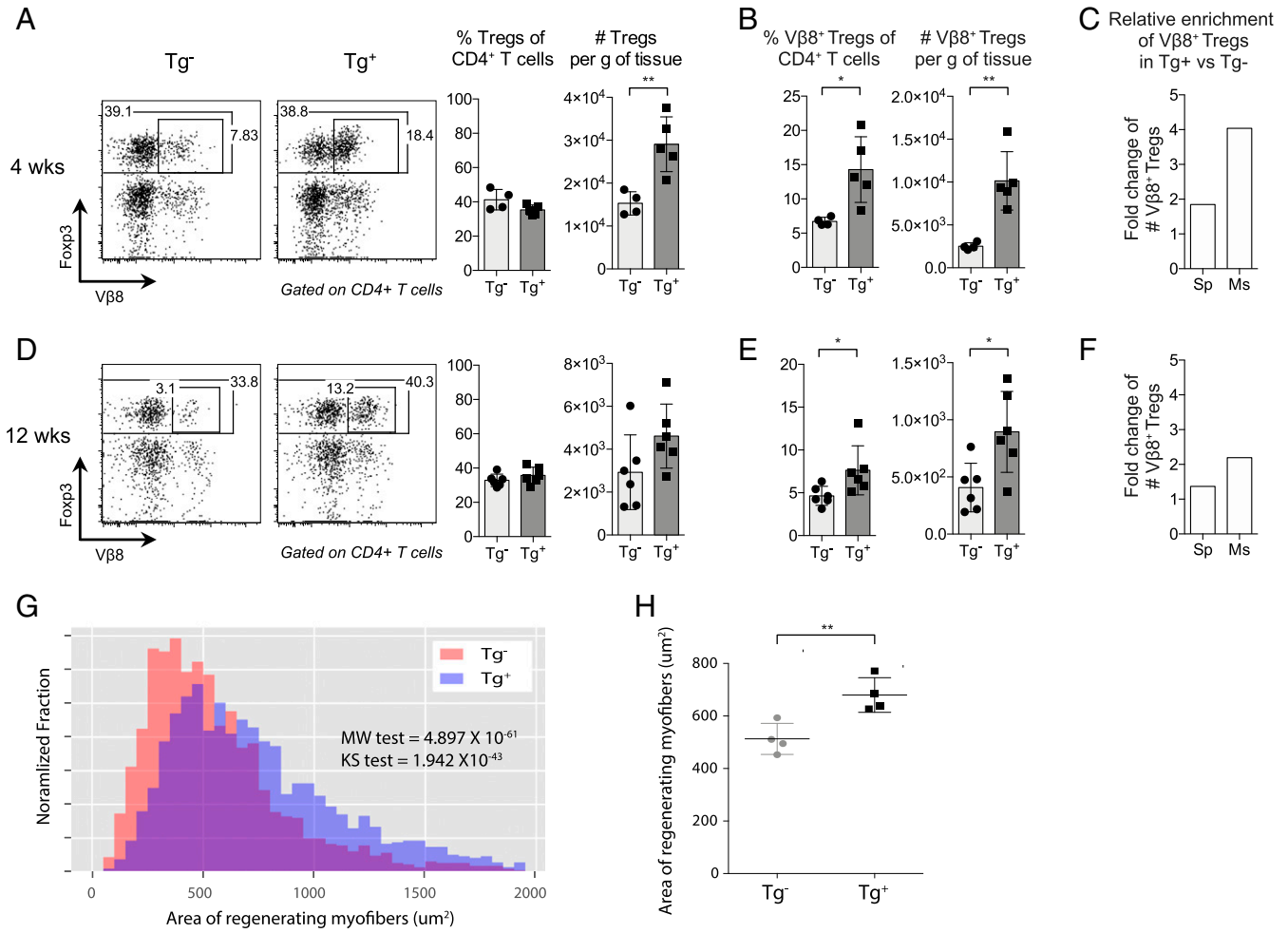

Fig. 4. An overabundance of Tregs expressing the mTreg24 specificity improved muscle regeneration in the *mdx* model. (*A–F*) Flow cytometric analyses. $CD4^+$ T cell compartments from muscles of Tg^- vs. Tg^+ *mdx* mice at 4 (*A–C*) or 12 (*D–F*) weeks of age. Statistics as per Fig. 1. $n = 6$. (*G* and *H*) Histologic analyses. Distribution (*G*) and mean (*H*) of cross-sectional area of regenerating myofibers from TA muscles of 12-wk-old Tg^- or Tg^+ *mdx* mice. Statistics as per Fig. 1 if not otherwise indicated. $*P < 0.05$, $**P < 0.01$.

Histology. TA muscles were fixed in Bouin's solution immediately after collection. Tissues were processed at the Rodent Histopathology Core of Harvard Medical School, as previously described (22). Images were acquired using a Nikon TE2000U inverted microscope and Zeiss Axio Imager M1 microscope. Quantitative analyses of the images were performed using FIJI software.

Statistical Analyses. Data were generally presented as mean ± SD. Most *P* values were calculated from the unpaired *t* test, using GraphPad Prism software. $*P < 0.05$; $**P < 0.01$; $***P < 0.001$, $****P < 0.0001$; *P* values for the volcano plots were calculated from the χ^2 test, using the Sci-Py package of Python. The Kolmogorov–Smirnov test and Mann–Whitney *U* test for the analyses of histology data were performed using the same tool.

Data Availability Statement: The data reported in this paper have been deposited in the Gene Expression Omnibus (GEO) database, https://www.ncbi.nlm.nih.gov/geo (accession no. GSE140419).

ACKNOWLEDGMENTS. We thank N. Asinovski, K. Hattori, Dr. A. Ortiz-Lopez, A. Cook, L. Yang, G. Buruzula, and A. Wood for experimental support; M. Panduro for helpful discussions; and Drs. B. Hanna and A. Mann for discussions and experimental help. Flow cytometry was performed at the Harvard Stem Cell Institute/Joslin Diabetes Center Core through grants P30DK036836 and S10OR021740. This work was funded by NIH Grant R01 AR070334 and by the JPB Foundation. J.C. and W.K. received fellowships from the National Research Foundation of the Ministry of Science, Information, Communication and Technology of South Korea (2016R1A6A3A03008459) and NIH (T32 GM007753 and F30 AG046045), respectively.

1. S. Z. Josefowicz *et al.*, Extrathymically generated regulatory T cells control mucosal TH2 inflammation. *Nature* **482**, 395–399 (2012).
2. M. Panduro, C. Benoist, D. Mathis, Tissue Tregs. *Annu. Rev. Immunol.* **34**, 609–633 (2016).
3. Y. Lavin, A. Mortha, A. Rahman, M. Merad, Regulation of macrophage development and function in peripheral tissues. *Nat. Rev. Immunol.* **15**, 731–744 (2015).
4. I. Amit, D. R. Winter, S. Jung, The role of the local environment and epigenetics in shaping macrophage identity and their effect on tissue homeostasis. *Nat. Immunol.* **17**, 18–25 (2016).
5. M. Feuerer *et al.*, Lean, but not obese, fat is enriched for a unique population of regulatory T cells that affect metabolic parameters. *Nat. Med.* **15**, 930–939 (2009).
6. D. Burzyn *et al.*, A special population of regulatory T cells potentiates muscle repair. *Cell* **155**, 1282–1295 (2013).
7. D. Kolodin *et al.*, Antigen- and cytokine-driven accumulation of regulatory T cells in visceral adipose tissue of lean mice. *Cell Metab.* **21**, 543–557 (2015).
8. D. Cipolletta *et al.*, PPAR-γ is a major driver of the accumulation and phenotype of adipose tissue Treg cells. *Nature* **486**, 549–553 (2012).
9. C. Li *et al.*, TCR transgenic mice reveal stepwise, multi-site acquisition of the distinctive fat-Treg phenotype. *Cell* **174**, 285–299.e12 (2018).
10. M. N. Wosczyna, T. A. Rando, A muscle stem cell support group: Coordinated cellular responses in muscle regeneration. *Dev. Cell* **46**, 135–143 (2018).
11. J. G. Tidball, Regulation of muscle growth and regeneration by the immune system. *Nat. Rev. Immunol.* **17**, 165–178 (2017).
12. W. Kuswanto *et al.*, Poor repair of skeletal muscle in aging mice reflects a defect in local, interleukin-33-dependent accumulation of regulatory T cells. *Immunity* **44**, 355–367 (2016).

13. S. A. Villalta *et al*., Regulatory T cells suppress muscle inflammation and injury in muscular dystrophy. *Sci. Transl. Med.* **6**, 258ra142 (2014).
14. J. R. DiSpirito *et al*., Molecular diversification of regulatory T cells in nonlymphoid tissues. *Sci. Immunol.* **3**, eaat5861 (2018).
15. E. Wakamatsu, D. Mathis, C. Benoist, Convergent and divergent effects of costimulatory molecules in conventional and regulatory $CD4^+$ T cells. *Proc. Natl. Acad. Sci. U.S.A.* **110**, 1023–1028 (2013).
16. A. G. Levine, A. Arvey, W. Jin, A. Y. Rudensky, Continuous requirement for the TCR in regulatory T cell function. *Nat. Immunol.* **15**, 1070–1078 (2014).
17. S. S. Chandran, C. A. Klebanoff, T cell receptor-based cancer immunotherapy: Emerging efficacy and pathways of resistance. *Immunol. Rev.* **290**, 127–147 (2019).
18. V. Kouskoff, H. J. Fehling, M. Lemeur, C. Benoist, D. Mathis, A vector driving the expression of foreign cDNAs in the MHC class II-positive cells of transgenic mice. *J. Immunol. Methods* **166**, 287–291 (1993).
19. J. Tuncel, C. Benoist, D. Mathis, T cell anergy in perinatal mice is promoted by T reg cells and prevented by IL-33. *J. Exp. Med.* **216**, 1328–1344 (2019).
20. S. Picelli *et al*., Full-length RNA-seq from single cells using Smart-seq2. *Nat. Protoc.* **9**, 171–181 (2014).
21. C. Trapnell *et al*., Differential gene and transcript expression analysis of RNA-seq experiments with TopHat and Cufflinks. *Nat. Protoc.* **7**, 562–578 (2012).
22. M. Panduro, C. Benoist, D. Mathis, T_{reg} cells limit IFN-γ production to control macrophage accrual and phenotype during skeletal muscle regeneration. *Proc. Natl. Acad. Sci. U.S.A.* **115**, E2585–E2593 (2018).